POLITECNICO DI TORINO
Repository ISTITUZIONALE

Inference of the size of nonlinear network systems from perceptible dynamics

Original
Inference of the size of nonlinear network systems from perceptible dynamics / Brovia, F.B., Zino, L., Succar, R., Porfiri, M.. - In: CHAOS. - ISSN 1054-1500. - STAMPA. - 36:2(2026). [10.1063/5.0318179]

Availability:
This version is available at: 11583/3007988 since: 2026-02-24T14:35:05Z

Publisher:
AIP Publishing

Published
DOI:10.1063/5.0318179

Terms of use:

This article is made available under terms and conditions as specified in the corresponding bibliographic description in the repository

Publisher copyright

(Article begins on next page)

06 November 2026

ACCEPTED MANUSCRIPT

Chaos
An Interdisciplinary Journal
of Nonlinear Science

This is the author's peer reviewed, accepted manuscript. However, the online version of record will be different from this version once it has been copyedited and typeset.
PLEASE CITE THIS ARTICLE AS DOI: 10.1063/5.0318179

AIP Publishing

Inference of the size of nonlinear network systems from perceptible dynamics

Francesca Bianca Brovia,[1,2,3,4] Lorenzo Zino,[4] Rayan Succar,[1,2] and Maurizio Porfiri*[1,2,5,6]
[1)]*Department of Mechanical and Aerospace Engineering, Tandon School of Engineering, New York University, Brooklyn NY, 11201, USA*
[2)]*Center for Urban Science and Progress, Tandon School of Engineering, New York University, Brooklyn NY, 11201, USA*
[3)]*Department of Applied Science and Technology, Politecnico di Torino, 10129 Turin, Italy*
[4)]*Department of Electronics and Telecommunications, Politecnico di Torino, 10129 Turin, Italy*
[5)]*Department of Biomedical Engineering, Tandon School of Engineering, New York University, Brooklyn NY, 11201, USA*
[6)]*Department of Civil and Urban Engineering, Tandon School of Engineering, New York University, Brooklyn NY, 11201, USA*

(*Electronic mail: mporfiri@nyu.edu)

(Dated: 15 January 2026)

Network dynamical systems are ubiquitous in science and engineering. The most basic property of a network dynamical system is its size, which, for scalar dynamics, corresponds to the number of nodes. For linear network systems, recent studies have developed reliable tools for inferring the size of the system from perceptible dynamics (measurements of one or some of the network nodes) across multiple experiments. Here, we extend these tools to nonlinear network systems by putting forward a model-agnostic approach that combines clustering techniques, detection matrices, and spectral analysis. The theoretical premise of the algorithm is that, under mild assumptions, the variation between the dynamics of some nodes across multiple measurements can be used to bound the variation between the dynamics of all nodes across the same measurements. By applying clustering techniques on perceptible dynamics, we identify nearby measurements, about which the variational dynamics are approximately linear and the use of the detection matrix is valid. From the spectrum of the detection matrix, we infer its rank, which corresponds to the size of the nonlinear network system. We demonstrate our approach via numerical experiments on different nonlinear network systems, including different types of hypergraphs. Whether nonlinearity comes from individual dynamics of the nodes or the interactions among them, it is rarely a feature that one can dismiss. Our work paves the way to infer the size of a nonlinear network system when governing equations are unknown and only limited data are accessible.

Research on the inference of interactions between the nodes of standard networks from their time-series is booming. We possess a powerful toolbox for detecting the strength and the direction of interactions, but for us to rely on it we must be able to confidently dismiss the possibility of hidden dynamics plaguing the inference. For linear network systems, there are ways to do that, but not for nonlinear systems. Say that we study the competition of two species in an ecological niche, how can we be sure that there is not a third one that is competing with both? In general, how can we tell the size of a nonlinear network system from the measurements of accessible nodes? Here, we provide a model-agnostic, theoretically grounded approach to address this open question. Our approach is expected to provide backing to existing literature on the inference of interactions between nodes of standard networks and open the door to research on the inference of interactions in hyper-networks —a wide open and enticing area of investigation.

I. INTRODUCTION

Two of the most fascinating problems in the history of science suggest that insights about nature's organization can be drawn from limited empirical observations. The first comes from Einstein's celebrated work on Brownian motion.[1] By studying trajectories of colloidal particles, Einstein was able to provide strong evidence for the atomic theory of matter and to estimate Avogadro's number. What appeared as random fluctuations turned out to reveal a universal constant, encapsulating how macroscopic data can encode hidden microscopic information. The second example comes from the seminal work of Maxwell[2], Boltzmann[3], and other pioneers of statistical mechanics, where ergodicity plays an important role[4]. By tracking a single particle in a real gas in time, one can infer the statistical properties of the entire ensemble, such as the Maxwell–Boltzmann distribution. This demonstrates how microscopic observations can translate into the macroscopic laws governing a system.

These examples point to a broader, unifying question: to what extent can we infer system-level dynamics from partial, noisy, or indirect observations? Tackling such questions lies at the heart of understanding network dynamical systems and the hidden structures that govern them. Network dynamical systems are a fundamental mathematical framework for modeling a wide variety of natural and technological phenomena that involve multiple interacting units, each one characterized by internal dynamics and interactions with others. Real-world internal dynamics and interactions are seldom linear. For instance, nonlinear network systems arise in neuro-

ACCEPTED MANUSCRIPT
Chaos
An Interdisciplinary Journal
of Nonlinear Science
AIP Publishing
This is the author's peer reviewed, accepted manuscript. However, the online version of record will be different from this version once it has been copyedited and typeset.
PLEASE CITE THIS ARTICLE AS DOI: 10.1063/5.0318179

science, where interactions beyond simple pairwise coupling shape brain functional networks[5–7]; in social systems, where behaviors are governed by higher-order social ties, such as collaborative networks[8–13]; and in biological dynamics, where nonlinear and higher-order processes influence the organization of microbiomes[14–17]. These multidisciplinary examples motivate the need for rigorous tools to investigate nonlinear network systems.

The most fundamental property of a network dynamical system is the size, which corresponds to the number of nodes in the case of scalar dynamics and, more in general, to the number of degrees of freedom for vectorial dynamics. Questions about the inference of the size of a system from limited measurements are pervasive in the natural sciences[18–22]. For instance, is it possible to determine the number of interacting species by observing the population trajectory of just a single species over time? Or, can we infer how many planets are in a system by observing the orbital motions of just a few of them? Several studies have recently attempted to answer these questions using different data-driven methods, including: i) the assembly of representative matrices from time-series measurements, whose rank reflects the size of the system[19,20,23]; ii) probing the system with specific input signals to observe its response[18]; and iii) estimating the diffusion coefficients of agents and relating them to the size of the collective[21].

Among these methods, the detection matrix has emerged as a simple and reliable tool[23], which is built using time-series from multiple measurements taken on one or multiple nodes. For linear, deterministic dynamics, the rank of this matrix is equal to the size of the system under mild assumptions; this claim holds whether or not the dynamics are autonomous or non-autonomous[19]. In the case of stochastic dynamics, such as Markov chains, one can construct a detection matrix that captures the evolution of probability distributions. This approach allows for the identification of the correct number of states in a Markov chain, even when some states are indistinguishable to the observer[24].

The detection matrix is conceptually related to the control-theoretic notion of observability[25]. Observability is a fundamental concept in control theory, as it connects a system's outputs to its internal states, determining whether those states can be reconstructed from available measurements. A system is said to be observable if all internal states can be estimated from the output measurements. For linear systems, this condition holds if and only if the rank of the so-called observability matrix is equal to the dimension of the system. Porfiri[19] demonstrated that, under mild assumptions, the rank of the detection matrix coincides with the rank of the observability matrix. To date, the application of the detection matrix to the nonlinear network systems remains limited and not fully understood. When it was first introduced by Haehne *et al.*[23], the method was successfully tested on periodic and chaotic oscillators through linearization in the phase space. The idea is to focus on a specific point in the phase space and examine the variation of nearby trajectories, which should be well described by linear dynamics. Although numerical results are promising, a theoretical guarantee is still lacking.

In this paper, we aim to address this gap by developing an algorithm that integrates concepts from nonlinear system theory and control theory to support the reliable use of the detection matrix for nonlinear network systems. We seek to infer the size of a nonlinear network system, in which nonlinearities may arise from internal dynamics or interactions. We are particularly keen towards hypergraph-based interactions, extending dyadic models that have dominated the literature on the inference of system size[18–20,23,24,26,27]. Hypergraphs are a generalization of standard graphs that allow edges to connect more than two nodes simultaneously. In a standard graph, an edge encodes an interaction between exactly two nodes. In contrast, a hyperedge in a hypergraph can link a set of nodes, capturing interactions that involve multiple participants at once. This framework is well suited to describe collective phenomena where outcomes depend on the joint state of several entities rather than pairwise relationships alone. Hypergraph-based models have recently attracted significant attention in the statistical physics, network science, and control communities[13,28–38], as they capture the complexity of real-world systems far more accurately than their dyadic counterparts. For example, in ecological systems, interactions often involve three or more species competing for shared resources or territory, while in social systems, collaboration networks frequently extend beyond pairwise relationships —such as in multi-author scientific publications, where a single paper may connect several researchers at once.

Toward achieving our objective, we establish a theoretical result that allows for bounding the distance between the state of a nonlinear system to a reference state using information only about the system output. Building on this result, we develop an algorithm that combines clustering techniques, detection matrices, and spectral analysis to infer the size of a nonlinear network system. For network systems with dense interactions, numerical experiments indicate that observing time-series from a single node may suffice to estimate the global network size precisely. Sparser networks require knowledge of more nodes, as one might expect. A key advantage of the proposed method lies in its model-agnostic nature, as it requires no assumptions about the underlying dynamics governing the system, making it broadly applicable to real-world settings where a mathematical model may not have been yet developed.

In summary, this paper contributes to the identification of the size of nonlinear network systems along two main directions. First, we establish a theoretical result that connects measurements at a single node —or, more generally, at a subset of nodes— to global state identification. Second, building on such a theoretical result, we propose a model-agnostic algorithm that estimates the network size from time-series of a subset of nodes by clustering nearby trajectories and building the detection matrix from the linearized dynamics.

The rest of the paper is organized as follows. Section II introduces the theoretical foundations required for the subsequent development of our method, which is detailed in Section III. Section IV presents numerical results on standard graphs and hypergraphs. Finally, conclusions are drawn in Section V.

ACCEPTED MANUSCRIPT
Chaos
An Interdisciplinary Journal
of Nonlinear Science
AIP Publishing
This is the author's peer reviewed, accepted manuscript. However, the online version of record will be different from this version once it has been copyedited and typeset.
PLEASE CITE THIS ARTICLE AS DOI: 10.1063/5.0318179

II. THEORY

A. Notation

We use the following notation. We denote real numbers as $\mathbb{R}$ and, given a positive integer N, we denote as $\mathbb{R}^N$ the N-dimensional Euclidean vector space. The 2-norm of vector $u \in \mathbb{R}^N$ is $\|u\| \coloneqq \sqrt{u^\top u}$, with $\top$ indicating vector and matrix transposition. Given a real matrix M, $\|M\|$ denotes the induced 2-norm, $\|M\| \coloneqq \sqrt{\rho(M^\top M)}$, where $\rho(M^\top M)$ is the spectral radius (the largest eigenvalue in magnitude). Given an m-dimensional, time-dependent vector $v(t)$, $v\colon [t_0, T] \to \mathbb{R}^m$, its L^2 norm on $\Omega \coloneqq [t_0, T]$

$$\|v\|_{L^2} \coloneqq \sqrt{\int_{t_0}^{T} \|v(\tau)\|^2 \,\mathrm{d}\tau}, \tag{1}$$

where t_0 and T denote the beginning and end of an observation throughout the paper.

B. Linearization and observability

We deal with nonlinear dynamical systems in the following form:

$$\dot{x}(t) = F(x(t)), \tag{2a}$$
$$y(t) = h(x(t)), \tag{2b}$$

where $x(t) \in \mathbb{R}^N$ is the state and $y(t) \in \mathbb{R}^n$ is the output, $\forall t \in \Omega$. The nonlinear vector fields $F\colon \mathbb{R}^N \to \mathbb{R}^N$ and $h\colon \mathbb{R}^N \to \mathbb{R}^n$ are assumed to be differentiable functions on their domain[39].

A widely used technique to analyze the dynamics of a nonlinear system is to linearize about a nominal trajectory $x^\star(t)$, thereby mapping the dynamics onto a linear time-varying (LTV) system[40]. We define the variation from the nominal trajectory as $\delta_x(t) \coloneqq x(t) - x^\star(t)$, and the variation of the output as $\delta_y(t) \coloneqq y(t) - y^\star(t)$, where $y^\star(t) = h(x^\star(t))$.

Nonlinear system (2) is locally approximated about the nominal trajectory $x^*(t)$ by LTV system

$$\dot{\delta}_x(t) = A(t)\delta_x(t), \tag{3a}$$
$$\delta_y(t) = C(t)\delta_x(t), \tag{3b}$$

where $A : \Omega :\to R^{N\times N}$ is the Jacobian matrix, $A(t) \coloneqq \left.\frac{\partial F(x)}{\partial x}\right|_{x^\star(t)}$, and $C : \Omega \to R^{n\times N}$ the output matrix, $C(t) \coloneqq \left.\frac{\partial h(x)}{\partial x}\right|_{x^\star(t)}$. In practical applications, we typically measure some of the network dynamical systems, so that function h in (2) is linear and the corresponding output matrix C is composed of zeros and ones —the latter corresponding to what we call perceptible dynamics.

The solution of linear system (3) is

$$\delta_x(t) = \Phi(t, t_0)\delta_x(t_0), \tag{4}$$

where the state transition matrix $\Phi : \Omega \times \Omega \to R^{N\times N}$ is computed from

$$\frac{\partial}{\partial t}\Phi(t, t_0) = A(t)\Phi(t, t_0), \tag{5a}$$
$$\Phi(t_0, t_0) = I, \tag{5b}$$

with I being the identity matrix. The solution of (5) is written in the form of Neumann series[41], which corresponds to the Dyson expansion in quantum physics and to the Peano–Baker series in control theory[42],

$$\Phi(t, t_0) = I + \int_{t_0}^{t} A(\tau)\,\mathrm{d}\tau + \int_{t_0}^{t}\int_{t_0}^{\tau_1} A(\tau_1)A(\tau_2)\,\mathrm{d}\tau_2\,\mathrm{d}\tau_1 + \dots \tag{6}$$

Consequently, the output can be expressed as

$$\delta_y(t) = C(t)\Phi(t, t_0)\delta_x(t_0). \tag{7}$$

Upon linearization, the system can be locally approximated by an LTV model, which allows us to apply classical concepts from linear systems theory. A system is said to be observable if one can uniquely reconstruct the initial state from the output over that window[42]. Observability can be analyzed through the observability Gramian

$$W(t_0, T) = \int_{t_0}^{T} \Phi^\top(t, t_0) C^\top(t) C(t) \Phi(t, t_0)\,\mathrm{d}t. \tag{8}$$

The system is said to be observable in Ω if and only if the symmetric matrix $W(t_0, T)$ is positive definite[42]; this condition ensures that no nontrivial initial state can generate identically zero output.

A slightly weaker notion of observability is structural observability[43]. For linear systems, structural observability depends on the sparsity pattern of the state transition matrix rather than on the specific numerical values of its entries[44] —the locations of zero and nonzero (fixed but otherwise arbitrary) entries. A system is said to be structurally observable if it is observable for almost all numerical assignments of the nonzero entries of the transition matrix. In particular, a fully connected system —one whose transition matrix has all entries nonzero— is structurally observable[45]. Intuitively, this is because information can propagate between any state variable and any potential sensor node. In what follows, we assume that the systems under consideration are observable. This assumption is reasonable, as the networks we study are connected, their coefficients are drawn randomly —as opposed to specific value that might hinder observability[43]— and self-loops are present —avoiding dynamics unfolding in low-dimensional space[46].

C. Bounding the internal state from the output

We consider nonlinear system (2), along with its linearized form (3), and we make the following assumptions.

ACCEPTED MANUSCRIPT
Chaos
An Interdisciplinary Journal
of Nonlinear Science
AIP Publishing
This is the author's peer reviewed, accepted manuscript. However, the online version of record will be different from this version once it has been copyedited and typeset.
PLEASE CITE THIS ARTICLE AS DOI: 10.1063/5.0318179

Assumption 1. *Matrix function A is piecewise continuous in Ω, so that*

$$\alpha := \operatorname*{ess\,sup}_{\tau\in[t_0,T]} \|A(\tau)\| \tag{9}$$

is well defined and Peano–Baker series (6) *satisfies*[47]

$$\|\Phi(t_1,t_2)\| \le e^{\alpha(t_1-t_2)}, \quad \forall t_1 \ge t_2. \tag{10}$$

Assumption 2. *Output matrix $C(t)$ is piecewise continuous in Ω.*

Assumption 3. *Observability Gramian matrix* (8) *is positive definite.*

Theorem 1. *Consider nonlinear system* (2)*, whose linearization about a nominal trajectory yields LTV system* (3)*. Under Assumptions 1–3, we have*

$$\|\delta_x(t)\| \le \frac{e^{\alpha(t-t_0)}}{\sqrt{\lambda_{\min}}} \|\delta_y\|_{L^2}, \tag{11}$$

where $\lambda_{\min}$ is the smallest eigenvalue of $W(t_0,T)$.

Proof. Recalling (4) and (7), we connect the L^2 norm of output δ_{y_i} to initial condition $\delta_x(t_0)$ through the observability Gramian,

$$\begin{aligned}\|\delta_y\|_{L^2}^2 &= \int_{t_0}^{T} (C(\tau)\Phi(\tau,t_0)\delta_x(t_0))^\top C(\tau)\Phi(\tau,t_0)\delta_x(t_0)\,\mathrm{d}\tau \\ &= \delta_x(t_0)^\top \left(\int_{t_0}^{T} \Phi(\tau,t_0)^\top C(\tau)^\top C(\tau)\Phi(\tau,t_0)\,\mathrm{d}\tau\right)\delta_x(t_0) \\ &= \delta_x(t_0)^\top W(t_0,T)\delta_x(t_0).\end{aligned} \tag{12}$$

Since the Gramian is symmetric and positive definite, all the eigenvalues are positive and Rayleigh's quotient is bounded by the smallest eigenvalue[42], that is,

$$\frac{z^\top W(t_0,t)z}{\|z\|^2} \ge \lambda_{\min}, \quad \forall z \in \mathbb{R}^N. \tag{13}$$

Combining (12) and (13) with $z = \delta_x(t_0)$, we bound the initial condition of the entire state using the L^2 norm of the output,

$$\|\delta_x(t_0)\| \le \frac{\|\delta_y\|_{L^2}}{\sqrt{\lambda_{\min}}}. \tag{14}$$

Next, we relate the initial condition of the state with the state at any time in Ω. Specifically, by applying Cauchy-Schwartz inequality and using the submultiplicativity of the norm[42], we establish

$$\frac{\mathrm{d}\|\delta_x(t)\|}{\mathrm{d}t} \le \|A(t)\|\|\delta_x(t)\|, \tag{15}$$

which, upon integration from t_0 to t, yields

$$\|\delta_x(t)\| \le \|\delta_x(t_0)\| + \int_{t_0}^{t} \|A(\tau)\|\|\delta_x(\tau)\|\,\mathrm{d}\tau. \tag{16}$$

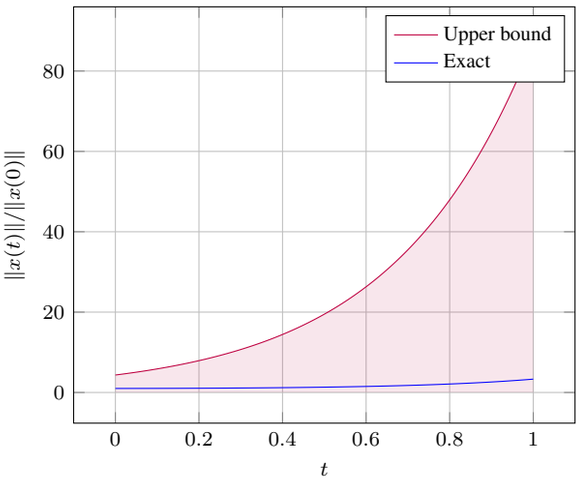


FIG. 1. Dynamics of Example 1. The red-shaded region represents the upper bound derived from Theorem 1, while the blue curve depicts the exact analytical solution of the system.

By using Grönwall-Bellman inequality[42] and Assumption 1, we obtain

$$\|\delta_x(t)\| \le \|\delta_x(t_0)\| e^{\alpha(t-t_0)}. \tag{17}$$

To prove the claim, we bound the norm of the initial condition in (17) using (14). □

The bound in (11) depends on the smallest eigenvalue of the observability Gramian, $\lambda_{\min}$, and the intrinsic system dynamics, encapsulated by α. The smaller $\lambda_{\min}$ (the larger α), the looser the bound.

We comment that the linearized dynamics in (3) and the associated transition matrix are linked to the variational equations commonly used in dynamical system theory[48,49], especially their asymptotics, which are used to estimate Lyapunov exponents for chaotic systems[50]. Here, instead, we leverage the transient information encoded in the transition matrix to assess the system's observability and infer its size.

Example 1. *We consider LTV system*

$$\dot{x}(t) = A(t)x(t), \qquad y(t) = Cx(t), \tag{18}$$

with

$$A = \begin{bmatrix} t+1 & -1 \\ -1 & t+1 \end{bmatrix}, \qquad C = \begin{bmatrix} 1 & 0 \end{bmatrix}. \tag{19}$$

The state-transition matrix is given by

$$\Phi(t,s) = e^{\frac{t^2-s^2}{2}+t-s} \begin{bmatrix} \cosh(t-s) & -\sinh(t-s) \\ -\sinh(t-s) & \cosh(t-s) \end{bmatrix}. \tag{20}$$

The system is observable over $[0,1]$, as Gramian

$$W(0,1) = \begin{bmatrix} 9.66 & -6.17 \\ -6.17 & 4.15 \end{bmatrix}, \tag{21}$$

ACCEPTED MANUSCRIPT
Chaos
An Interdisciplinary Journal
of Nonlinear Science
AIP Publishing
This is the author's peer reviewed, accepted manuscript. However, the online version of record will be different from this version once it has been copyedited and typeset.
PLEASE CITE THIS ARTICLE AS DOI: 10.1063/5.0318179

is positive definite with $\lambda_{\min} = 0.144$. We can calculate bound in Theorem 1, by noting that $\alpha = 3$; see Fig. 1 for a comparison between the evolution of the state norm and the theoretical bound.

III. METHODOLOGY

Here, we describe our methodology to infer the size of a nonlinear network system from perceptible dynamics (Algorithm 1), illustrated in Fig. 2. We assume we have access to M independent measurements, which may come from multiple experiments in which the researcher can initiate the dynamics from different initial conditions, or a single one in which they partition a longer observation into shorter segments[26,27]. Each measurement consists of the discrete-time recording of the output of a subset of n nodes at S sampling times, all contiguous in time, which we denote as $\{y^{(i,\ell)}(t_j)\}$, for nodes $i = 1,\dots,n$, experiments $\ell = 1,\dots,M$, and sampling times $t_1,\dots,t_S$. In the rest of the paper, we assume that the output of the generic i-th node at time t_j is a scalar quantity, $y^{(i,\ell)}(t_j) \in \mathbb{R}$. This allows us to maintain a simple notation without loss in generality. In fact, one can deal with vectorial nodal outputs by simply considering each entry as a distinct duplicate of the same node, ultimately obtaining an estimate of the number of degrees of freedom in the system; see, for instance, Celli and Porfiri [26] for linear systems.

The first step of our approach consists in the partition of the M measurements into K clusters of nearby dynamics. Based on Theorem 1, one can argue that two measurements with close perceptible dynamics will also have nearby evolution of the internal state of the network system. Hence, measurements within a cluster can be viewed as variations around a nominal trajectory, described by a linearized model that can be studied using a detection matrix. In particular, we apply the standard K-means algorithm to minimize the objective function $\sum_{k=1}^{K}\sum_{\ell\in\mathscr{Y}_k}\sum_{i=1}^{n}\sum_{j=1}^{S}|y^{(i,\ell)}(t_j)-\mu_{k,j}^{(i)}|^2$ over the set of clusters $\mathscr{Y} = \{\mathscr{Y}_1,\dots,\mathscr{Y}_K\}$, where $\mu_{k,j}^{(i)} \in \mathbb{R}$ is the mean of $y^{(i,\ell)}(t_j)$'s over the measurements $\ell \in \mathscr{Y}_k$[51] (see Line 1 of Algorithm 1). A relatively small value of K is preferred to avoid artificially shrinking the intra-cluster distance. When dealing with a broad range of initial conditions and a larger ensemble of measurements, one may consider increasing K to refine the local characterization of the dynamics. If a cluster contains less than $S+1$ measurements, we discard it from the analysis, so that we work with the $\hat{K}$ clusters that have at least $S+1$ measurements, $\hat{\mathscr{Y}}$ (see Line 2 of Algorithm 1).

The second step is to construct a detection matrix for each cluster. Given our ultimate goal of aggregating inferences from all the detection matrices into a single estimate, we proceed as follows. If the cluster contains more than $S+1$ measurements, we prune the cluster to $S+1$ measurements by eliminating the measurements that are the furthest away from the mean over the length of the measurement. In particular, for each trajectory $\ell \in \mathscr{Y}_k$, we compute $d^{(\ell)} = \sum_{i=1}^{n}\sum_{j=1}^{S}|y^{(i,\ell)}(t_j)-\mu_{k,j}^{(i)}|^2$ and eliminate trajectories with the largest values of $d^{(\ell)}$ (see Lines 4–5 of Algorithm 1). For notational convenience, we assume that trajectories are ordered so that the closest to the mean are the first $S+1$.

The third step is to identify the trajectory that is the closest to the mean in each of the retained and pruned clusters, that is, the trajectory with the smallest $d^{(\ell)}$. Such a trajectory is regarded as the nominal trajectory for cluster $\mathscr{Y}_k$, denoted as $\hat{y}_k$, and it is used to define the variational dynamics within the cluster at each time-step t_j, $j = 1,\dots,S$, denoted as $\delta y^{(\ell)}(t_j) \in \mathbb{R}^n$, which is a vector whose generic i-th entry is equal to the difference $y^{(i,\ell)}(t_j) - \hat{y}_k^{(i)}(t_j)$ (see Line 6 of Algorithm 1). We do not use the centroid itself as the nominal trajectory because, in nonlinear systems, superposition principle does not hold. Consequently, cluster centroids generally do not satisfy the system dynamics and cannot serve as valid nominal trajectories.

The fourth step entails the assembly of the detection matrix[19,23] of cluster $\mathscr{Y}_k$ (see Line 7 of Algorithm 1)

$$\mathscr{T}_k = \begin{bmatrix} \delta y^{(1)}(t_1) & \delta y^{(2)}(t_1) & \cdots & \delta y^{(S)}(t_1) \\ \delta y^{(1)}(t_2) & \delta y^{(2)}(t_2) & \cdots & \delta y^{(S)}(t_2) \\ \vdots & \vdots & \ddots & \vdots \\ \delta y^{(1)}(t_S) & \delta y^{(2)}(t_S) & \cdots & \delta y^{(S)}(t_S) \end{bmatrix}. \tag{22}$$

Columns encode the temporal evolution of distinct trajectories, while rows represent time across trajectories.

Then, we estimate the rank of the detection matrix (see Line 8 of Algorithm 1), which for observable LTVs, is equal to the size of the system[19]. To estimate the rank, we follow the method proposed in Haehne *et al.* [23], which identifies the rank as the index of the largest gap in the ordered singular value spectrum, computed on the logarithmic scale as $\Delta_s = \log(\sigma_s) - \log(\sigma_{s+1})$, for $s \in \{1,...,S-1\}$. The spectral gap allows for separating large singular values associated with system dynamics from small ones those due to the linear approximation and noise (see Lines 8–9 of Algorithm 1).

Finally, the size of the nonlinear network system is estimated as the average rank over the different clusters $\hat{N}$ (see Line 11 of Algorithm 1).

ACCEPTED MANUSCRIPT
Chaos
An Interdisciplinary Journal
of Nonlinear Science
AIP Publishing
This is the author's peer reviewed, accepted manuscript. However, the online version of record will be different from this version once it has been copyedited and typeset.
PLEASE CITE THIS ARTICLE AS DOI: 10.1063/5.0318179

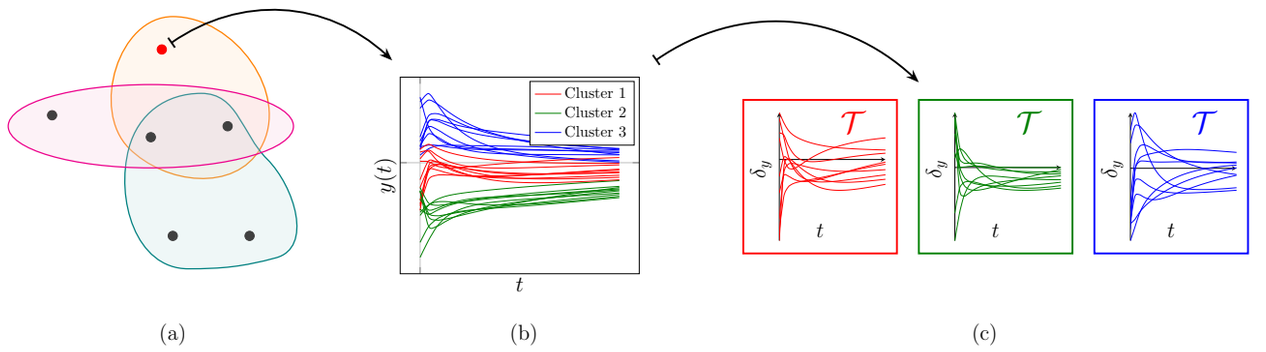


FIG. 2. Schematic illustration of our approach. (a) Network of $N = 6$ nodes, where one node (red point) is accessible. (b) Time-series of the perceptible dynamics, from different initial conditions. (c) Trajectories are clustered in three groups; different colors are associated with different clusters. A detection matrix is assembled for each cluster to solve the inference problem.

Algorithm 1 Network size estimation

Require: Nonlinear system (black box), n accessible nodes, M measurements, S recordings per measurement
Ensure: Estimated system size $\hat{N}$

Apply K-means clustering at each time-step to partition the set of measurements into K clusters.
Remove clusters with less than $S+1$ elements, keeping $\hat{K}$ clusters, termed $\{\mathscr{Y}_1,\dots,\mathscr{Y}_{\hat{K}}\}$
for each cluster $k = 1,\dots,\hat{K}$ **do**
    Compute $d^{(\ell)} = \sum_{i=1}^{n}\sum_{j=1}^{S}|y^{(i,\ell)}(t_j) - \mu_{k,j}^{(i)}|^2$.
    Select the $S+1$ nearest trajectories to the cluster mean
    Select the nominal trajectory $\hat{y}_k$ as the trajectory that is closest to the cluster mean.
    Construct the detection matrix $\mathscr{T}_k$ using (22).
    Compute singular value decomposition
    Identify largest spectral gap and draw the size estimate for the cluster, $\hat{N}_k$
end for
Compute estimate $\hat{N} = \frac{1}{\hat{K}}\sum_{k=1}^{\hat{K}}\hat{N}_k$

IV. RESULTS

Here, we demonstrate the proposed method by performing a series of numerical experiments on different classes of nonlinear network systems. The aim is threefold. First, we verify the accuracy of the estimated system size with respect to the true dimension. Second, we evaluate the robustness of the method against parameter changes. Third, we demonstrate the applicability of the approach across different model systems, including hypergraph-based systems.

A. Model systems

A hypergraph $H = (V,E)$ is a generalization of a standard graph where $V = \{1,\dots,N\}$ is the set of nodes and E is the set of hyperedges, each of which can connect any number of vertices. A k-uniform hypergraph is a special case where each and every hyperedge contains exactly k vertices. In a compact form, hyperedges can be represented by a family of adjacency tensors $A^{(p)}$, $p = 2,3,\dots$, which determine which p-tuple of nodes are connected. In other words, the entry $a^{(p)}_{ijk\dots\ell}$ of $A^{(p)}$ is non-zero if the p-tuple $\{i,j,k,\dots,\ell\}$ is connected by an hyperedge, and its magnitude determines the strength of such a connection. Standard graphs can be interpreted as 2-uniform hypergraphs, where the adjacency tensors reduce to the standard adjacency matrix. Assuming scalar dynamics for each node, we write[38]

$$\dot{x}_i(t) = f_i(x_i(t)) + \sum_{j=1}^{N} a^{(2)}_{ij}\, h^{(2)}(x_i(t),x_j(t)) + \sum_{j,k=1}^{N} a^{(3)}_{ijk}\, h^{(3)}(x_i(t),x_j(t),x_k(t)) + \dots, \qquad (23)$$

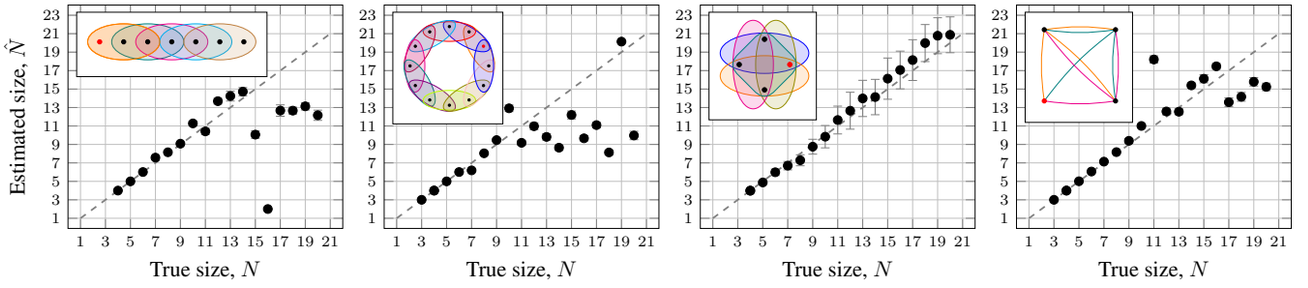
for $i = 1,\dots,N$, where f_i describes the intrinsic dynamics of node i. Interaction function $h^{(p)}$ captures the functional form through which multiple nodes belonging to a hyperedge collectively influence each other. We consider four representative instances of (23) that illustrate different structural and dynamical features.

Example 2 (Linear hyperchain). *In the linear hyperchain, a system of N nodes evolves according to linear internal dynamics ($f_i(x_i) = a_i x_i$) and nearest-neighbor interactions. We consider a third-order hyperchain, where each node interacts with the node before and after, except for the first node that interacts with the second and third and the last one that interacts with the second and third last. Hence, the dynamics of each node depend only on the states of its neighbors along a chain, yielding the following equations:*

$$\begin{cases} \dot{x}_1(t) = a_1 x_1(t) + a^{(2)}_{1,2,3} x_2(t) x_3(t), \\ \dot{x}_i(t) = a_i x_i(t) + a^{(2)}_{i-1,i,i+1} x_{i-1}(t) x_{i+1}(t), \quad i = 2,\dots,N-1, \\ \dot{x}_N(t) = a_N x_N(t) + a^{(2)}_{N,N-1,N-2} x_{N-2}(t) x_{N-1}(t). \end{cases} \qquad (24)$$

This simple topology allows us to test the performance of the algorithm in a setting where the interaction pattern is minimal and local. Note that, while the internal dynamics is linear, nonlinearities arise from the coupling terms.

ACCEPTED MANUSCRIPT
Chaos
An Interdisciplinary Journal
of Nonlinear Science
AIP Publishing
This is the author's peer reviewed, accepted manuscript. However, the online version of record will be different from this version once it has been copyedited and typeset.
PLEASE CITE THIS ARTICLE AS DOI: 10.1063/5.0318179



(a) Linear hyperchain (b) Linear hypercycle (c) LW 3-4 complete hypergraph (d) Quadratic standard graph

FIG. 3. Inference of network size from measurements at single node. For each model (a–d), a marker represents the mean estimate across 100 independent realizations; vertical error bars indicate one standard deviation. The bisectrix (dashed gray) serves as a visual reference of perfect inference. In the inferences, we use $M = 1,000$ trajectories, $K = 2$ clusters, and (a,b) $S = 25$ or (c,d), $S = 30$ time-steps. Measured nodes are marked in red.

Example 3 (Linear hypercycle). *A closely related model to the hyperchain is the hypercycle, obtained by imposing periodic boundary conditions to the linear hyperchain. In this case, the last node is coupled again to the first one, resulting in a cyclic structure. The hypercycle provides a slightly more complex configuration than the hyperchain, as it introduces long-range coupling through the closure of the loop, while still maintaining a regular and homogeneous topology. The evolution of the system over time is described by the following ordinary differential equation:*

$$\dot{x}_i(t) = a_i x_i(t) + a^{(2)}_{i-1,i,i+1} x_{i+1}(t) x_{i-1}(t), \qquad i = 1,\dots,N, \tag{25}$$

where cyclic boundary conditions are applied, that is, $N \equiv 0$ and $N+1 \equiv 1$.

Example 4 (Linear weighted 3-4 complete hypergraph). *In this example, we focus on interactions of order three and four, corresponding to three-body and four-body terms, respectively,*

$$\dot{x}_i(t) = a_i x_i(t) + \sum_{j,k=1}^{N} a^{(2)}_{ijk} x_j(t) x_k(t) + \sum_{j,k,l=1}^{N} a^{(3)}_{ijkl} x_j(t) x_k(t) x_l(t). \tag{26}$$

This model captures more intricate dependencies than the previous ones, since higher-order terms regulate how groups of three nodes collectively influence one another. It is particularly suitable for testing the capacity of the method to handle higher-order interactions.

Example 5 (Quadratic standard graph). *Finally, we investigate a scenario where the nodes interact over a standard graph —only interactions of order two are present— but internal dynamics and coupling terms feature quadratic terms. We rewrite the dynamics using coefficients a_{ij} and b_{ij}, which are the matrix entries of matrices A and B, to capture quadratic and linear couplings between node i and node j, respectively (the terms a_{ii} and b_{ii} capture the corresponding terms in the internal dynamics). Matrix A weights the local quadratic terms x_j^2 and is chosen to be diagonal with strictly negative entries, thereby inducing dissipative nonlinear self-dynamics at each node. Matrix B encapsulates the linear coupling among nodes and is symmetric and negative definite, ensuring the stability of linear dynamics. Ultimately, we write the following equation set:*

$$\dot{x}_i(t) = \sum_{j=1}^{N} a_{ij} x_j(t)^2 + \sum_{j=1}^{N} b_{ij} x_j(t), \qquad i = 1,\dots,N. \tag{27}$$

This example is representative of nonlinear network systems based on standard dyadic interactions between the nodes.

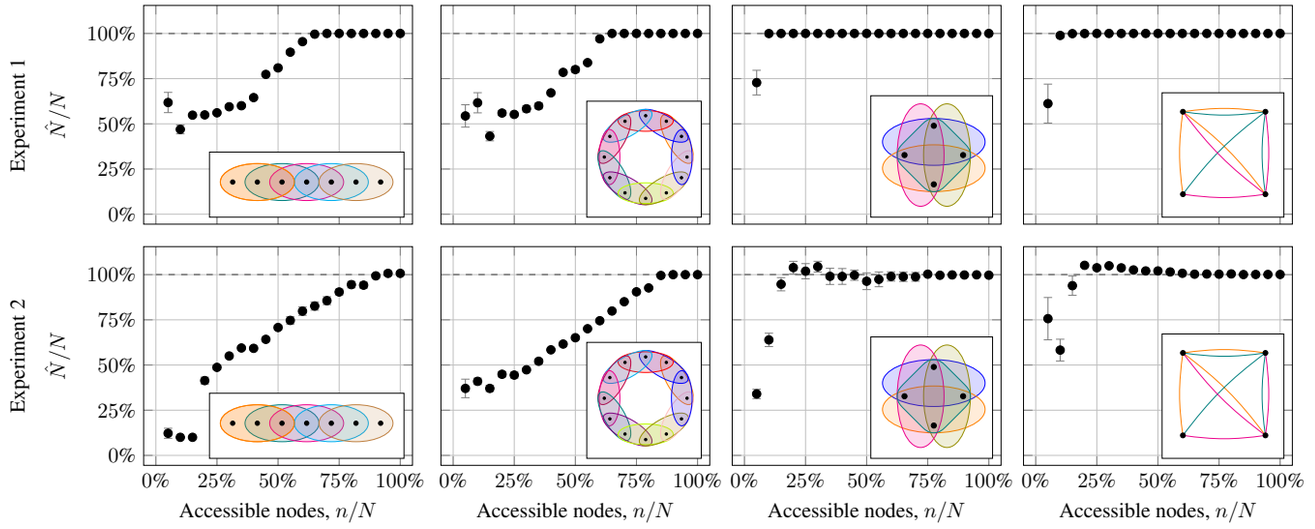
Together, these four classes of models span a spectrum of structural complexity, from simple chains to fully connected higher-order hypergraphs, providing a comprehensive benchmark for the proposed method.

B. Inference from a single node

To gather statistical insight, we work with 100 realizations of the model systems. For the hyperchain (Example 2), a_i and a_{ij} are sampled uniformly at random in $\{-1, -0.9, -0.8\}$ and $\{-5.5, -5.0, -4.5, 4.5, 5.0, 5.5\}$, respectively. For the hypercycle (Example 3), a_i and $a_{i-1,i,i+1}$ are sampled uniformly at random in $\{-1.8, -1.7\}$ and $\{-4.5, -4.0, -3.5, 3.5, 4.0, 4.5\}$, respectively. For the linear weighted (LW) 3-4 complete hypergraph (Example 4), a_i is sampled uniformly at random in $\{-0.05, -0.04, -0.03, -0.02\}$, while a_{ijk} and a_{ijkl} are sampled uniformly at random in $\{-0.005, -0.002, 0.005, 0.002\}$. For the quadratic standard graph (Example 5), A is a diagonal matrix with each entry sampled uniformly at random in $\{-1.5, -0.5\}$ and $B = -(M^\top M + \mu I)$, with the each entry of matrix M sampled from a normally distributed random variable with 0 mean and unit variance, and $\mu = 0.5$, in order to have a negative definite matrix. The initial conditions are sampled uniformly at random in $[0.5 - 10^{-5}, 0.5 + 10^{-5}]$. Without loss of generality, node 1 is the accessible one. Each trajectory is simulated for a time interval of unit length and sampled with a uniform spacing, unless differently specified.

In agreement with our intuition, measurements from a single node are sufficient to accurately infer the size of a nonlinear network system of a small size (Fig. 3). Across multiple

ACCEPTED MANUSCRIPT
Chaos
An Interdisciplinary Journal
of Nonlinear Science
AIP Publishing
This is the author's peer reviewed, accepted manuscript. However, the online version of record will be different from this version once it has been copyedited and typeset.
PLEASE CITE THIS ARTICLE AS DOI: 10.1063/5.0318179



(a) Linear hyperchain (b) Linear hypercycle (c) LW 3-4 complete hypergraph (d) Quadratic standard graph

FIG. 4. Inference of network size from measurements at multiple nodes. We plot $\hat{N}/N$ versus the fraction of selected nodes n/N; markers show averages over 100 independent realizations and error bars denote one standard deviation. The number of nodes is $N = 20$. In the inferences, we use $M = 1,000$ trajectories, $K = 2$ clusters, and (a,b) $S = 25$ or (c,d), 30 time-steps. Two sets of experiments are performed with different ranges of initial conditions: for Experiment 1 (first row), initial states are uniformly sampled in $[0.5 - 10^{-5}, 0.5 + 10^{-5}]$, for Experiment 2 (second row) they are uniformly sampled in $[0.5 - 10^{-2}, 0.5 + 10^{-2}]$. Insets show the corresponding interaction topologies.

model systems, we demonstrate the possibility of inferring the system size for networks with less than 10 nodes. Whether the nonlinearity is due to the interaction, as in a hypergraph-based model, or in the internal dynamics, as in the standard graph, our methodology yields accurate predictions of the system size. As the network size increases past 10 nodes, consistent recovery from a single-node measurement is only possible for complete hypergraphs. In this case, any node contains a significant footprint of the whole network, thereby enriching the information contained in the detection matrix.

C. Inference from multiple nodes

The setup for the simulation is equivalent to the one presented above, with the main difference being that more than one node are accessible. Without loss of generality, we assume that the first n/N nodes are accessible. Also different from the analysis above, we consider two sets of initial conditions: sampling at random in $[0.5 - 10^{-5}, 0.5 + 10^{-5}]$ (Experiment 1) and sampling at random in $[0.5 - 10^{-2}, 0.5 + 10^{-2}]$ (Experiment 2).

Measuring more than one node opens the door for accurate inferences of larger systems (Fig. 4). In agreement with our intuition, size recovery improves in a nearly monotonic fashion as the number of measured nodes increases. The more information is collected from the network, the closer is our estimate to the true system size. Across model systems, measurements of about a half of the network nodes seem to be sufficient to exactly determine the system size. Yet, for dense networks, such as complete hypergraphs or quadratic standard graphs, even 10% of the nodes are sufficient to achieve exact size recovery. In contrast, for sparse topologies such as chains or cycles, a larger number of measured nodes is required before the system size can be reliably identified. These results highlight how the structural properties of a network influence the amount of information that shall be sampled in order to achieve accurate inference.

These conclusions are fairly robust to changes in the range of the initial conditions (Fig. 4). Widening the initial conditions by three orders of magnitude yields some reductions in the accuracy of the inference. Specifically, for the linear hyperchain and the linear hypercycle, one needs to increase the fraction of accessible nodes to 80% to attain perfect inference. With respect to the LW 3-4 complete hypergraph and the quadratic standard graph, performance deteriorates marginally. In these cases, 15% of the network nodes are needed for a perfect inference, offering promise for the application of the methodology beyond synthetic data.

D. Robustness analysis

To demonstrate the dependence of our findings with respect to the parameters of the algorithms, we perform additional simulations on the most challenging case examined above (Fig. 4a), namely, the linear hyperchain in Experiment 2. We individually vary (doubling) the number of time-steps S, the number of trajectories M, and the number of clusters K compared to the case in in Figure 4. Overall, we do not unveil a critical effect of S and M (Figs. 5a–5b), warning prudence against embarking in higher computational costs

ACCEPTED MANUSCRIPT
Chaos
An Interdisciplinary Journal
of Nonlinear Science
AIP Publishing
This is the author's peer reviewed, accepted manuscript. However, the online version of record will be different from this version once it has been copyedited and typeset.
PLEASE CITE THIS ARTICLE AS DOI: 10.1063/5.0318179

with longer time-series or more measurements. Increasing the number of clusters K to four seems to have a more beneficial effect, whereby we attain nearly perfect inference by measuring about 70% of the network, instead of the 80% mark required when using two clusters (Fig. 5c). This evidence is in line with our intuition that a small number of clusters may be inadequate to describe dynamics with wider initial conditions.

We also test the performance of our algorithm on a larger network. Specifically, we consider a network with $N = 100$ nodes, and we repeat the analysis performed in Section IV C for the quadratic standard graph (Example 5). Our results (Fig. 6), are consistent with our findings for smaller networks in Fig. 4d, suggesting that our algorithm can also be applied to larger networks. In fact, our numerical simulations (Fig. 6) reveal that it is enough to access 17% of the nodes to obtain the correct estimate of the network size N.

Finally, we test the robustness of our method with respect to the presence of noise in the measurements. Specifically, we consider the scenario of the linear hyperchain in Experiment 1 (Fig. 4a, top row), and simulate an additive Gaussian noise on the measurement. Specifically, each measurement $y^{(i,\ell)}(t_j)$ is defined as the sum of the value of the output of node i at time t_j in experiment ℓ and the realization of a Gaussian with 0 mean and different standard deviations, each realization independent of the others. For our analysis, we consider three different values of standard deviation, defined in relative terms with respect to the average value of the state, denoted as ε_{rel}. Our results (Fig. 7), suggest that our method is robust with respect to small-to-medium levels of noise. For noise with relative standard deviation $\varepsilon_{\text{rel}} < 1\%$ with respect to the value of the state, the results obtained are almost indistinguishable from those obtained in the absence of noise, with a visible but slight worsening of the inference quality when $\varepsilon_{\text{rel}} = 1\%$. Importantly, the algorithm does not seem to tend to overestimate the network size.

V. CONCLUSION

Recent years have seen a surge of methodologies to estimate the size of a network dynamical system from perceptible dynamics[18–24,26,27]. Most of the research has focused on linear network systems, hindering application to real-world systems where nonlinearities arise from internal dynamics and coupling. The latter case is one that is becoming more and more timely, as hypergraphs are gaining traction[5,13,22,28–38]. To address this methodological gap, we put forward a novel methodology that leverages time-series from accessible nodes across multiple experiments.

Our approach unfolds in a sequence of algorithmic steps, which start from clustering analysis of available trajectories to inform the identification of close-by dynamics for the entire state. For each cluster, we construct a detection matrix, encoding the evolution of the variational dynamics about the cluster mean trajectory. By computing the rank of all the detection matrices, we estimate the size of the system. Knowledge of a single network node is sufficient to determine the size of dense networks, where the dynamics of each node contains a footprint of the entire network. For sparse networks, instead, one may need to rely on a more complete knowledge of the system dynamics, unless the network contains less than ten nodes.

The main limitations of our work are its reliance on the observability of the nonlinear network systems —a property that is not universal to all network systems. For example, structured networks without self-loops may fail to display observability[52,53]. Beyond the relaxation of the assumption of observability, several extensions are promising. First, an exact quantification of the role of network density on the algorithm success is lacking. While we numerically document a difference between sparse and dense networks, we lack a theoretical lens to examine such a difference. Second, our validation focuses on non-divergent dynamics and to a limited set of parameters. Performing an extensive numerical parametric study as well as further simulations on other scenarios —including vectorial dynamics— is an important direction of future research. Third, we presently rely on a the mean rank of the detection matrix across clusters; it is tenable that further insight could be gathered by examining the variations across clusters, especially when dealing with experimental trajectories that are best described by several clusters. Fourth, the algorithm assumes deterministic dynamics, while numerical simulations suggest that the proposed method is robust with respect to small-to-medium levels of noise. Formally extending the approach to account for stochasticity in the form of added noise or network dynamics is an important area of research.

In conclusion, this work opens a pathway to model-agnostic inference of hidden dynamics in nonlinear networked dynamics. Without prior knowledge of governing equations, our approach promises wide applications in science and engineering.

ACKNOWLEDGMENTS

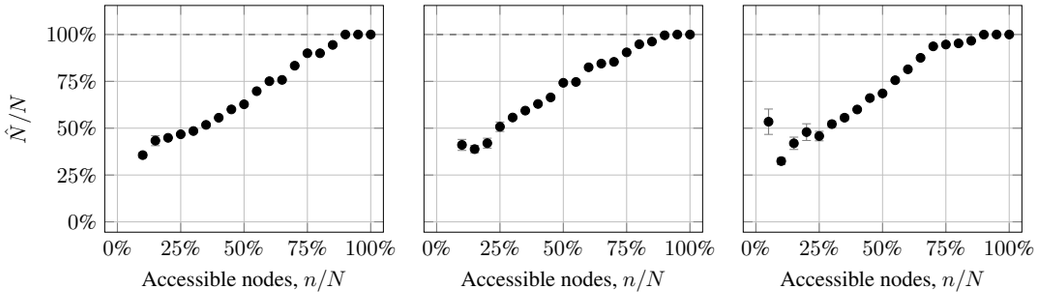
The work by F.B. Brovia, R. Succar, and M. Porfiri was supported by the National Science Foundation under grant no. CMMI-1953135. The work by L. Zino was carried out within FAIR (Future Artificial Intelligence Research) and received funding from the European Union Next-GenerationEU (PIANO NAZIONALE DI RIPRESA E RESILIENZA (PNRR) — MISSIONE 4 COMPONENTE 2, INVESTIMENTO 1.3 — D.D. 1555 11/10/2022, PE00000013). This manuscript reflects only the authors' views and opinions, neither the National Science Foundation, nor the European Union or the European Commission can be considered responsible for them.

AUTHORS DECLARATION

Conflict of Interest Statement

The authors have no conflicts to disclose.

ACCEPTED MANUSCRIPT
Chaos
An Interdisciplinary Journal
of Nonlinear Science
AIP Publishing
This is the author's peer reviewed, accepted manuscript. However, the online version of record will be different from this version once it has been copyedited and typeset.
PLEASE CITE THIS ARTICLE AS DOI: 10.1063/5.0318179



(a) S=50 (b) M=2,000 (c) K=4

FIG. 5. Inference of system size from multiple perceptible dynamics for hyperchain with varying parameters. We plot $\hat{N}/N$ versus the fraction of selected nodes n/N; markers show averages over 100 independent realizations and error bars denote one standard deviation. Unless differently stated in the sub-caption, $N = 20$, $S = 25$, $M = 1{,}000$, and $K = 2$. Initial states are uniformly sampled in $[0.5 - 10^{-2}, 0.5 + 10^{-2}]$.

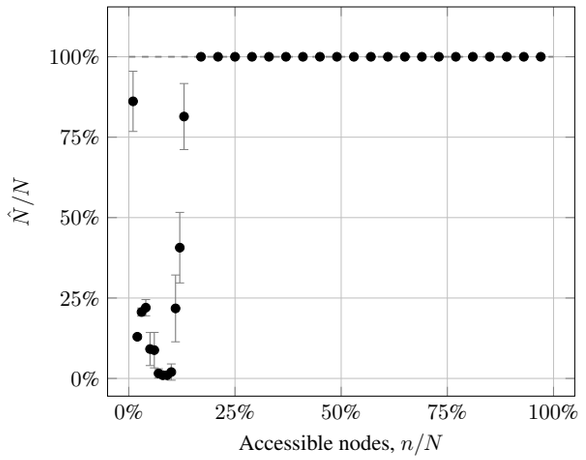


FIG. 6. Inference of system size from multiple perceptible dynamics for quadratic standard graph with $N = 100$. We plot $\hat{N}/N$ versus the fraction of selected nodes n/N; markers show averages over 100 independent realizations and error bars denote one standard deviation. In the inferences, we use $M = 4{,}000$ trajectories, $K = 2$ clusters, and $S = 110$. Each trajectory is simulated for a time interval of $[0.0, 0.75]$. Initial states are uniformly sampled in $[0.5 - 10^{-5}, 0.5 + 10^{-5}]$.

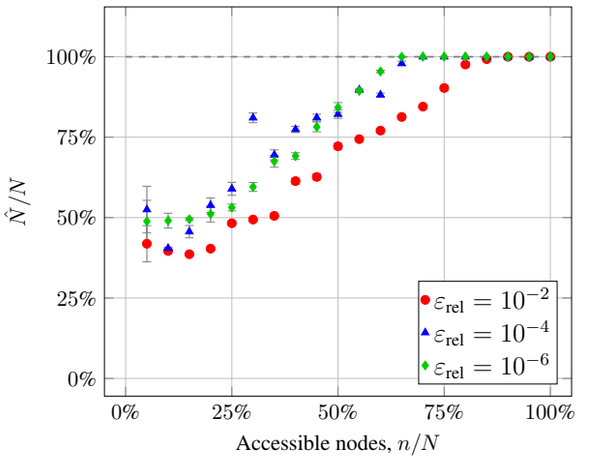


FIG. 7. Inference of system size from multiple nodes for hyperchain with different colors representing different levels of noise, ε_{rel}. We plot $\hat{N}/N$ versus the fraction of selected nodes n/N; markers show averages over 100 independent realizations and error bars denote one standard deviation. The number of nodes is $N = 20$. In the inferences, we use $M = 1{,}000$ trajectories, $K = 2$ clusters, and $S = 25$. Initial states are uniformly sampled in $[0.5 - 10^{-5}, 0.5 + 10^{-5}]$.

Data Availability Statement

The data that support the findings of this study and the code used for the simulations is available at `https://github.com/dynamicalsystemslaboratory/dynamics-size-inference`

Author Contributions

Francesca Bianca Brovia: Data Curation, Formal Analysis, Investigation, Methodology, Project Administration, Software, Validation, Visualization, Writing — Original Draft Preparation. **Rayan Succar:** Investigation, Methodology, Writing — Review & Editing. **Lorenzo Zino:** Conceptualization, Investigation, Methodology, Supervision, Writing — Review & Editing. **Maurizio Porfiri:** Conceptualization, Funding Acquisition, Investigation, Methodology, Resources, Supervision, Writing — Review & Editing.

[1] A. Einstein, "Über die von der molekularkinetischen theorie der wärme geforderte bewegung von in ruhenden flüssigkeiten suspendierten teilchen," Annalen der Physik **322**, 549–560 (1905).
[2] J. C. Maxwell, "On the dynamical theory of gases," Philosophical Transactions of the Royal Society of London , 49–88 (1867).
[3] L. Boltzmann, "Weitere studien über das wärmegleichgewicht unter gasmolekülen," in *Kinetische Theorie II: Irreversible Prozesse Einführung und Originaltexte* (Springer, 1970) pp. 115–225.
[4] M. Baldovin, R. Marino, and A. Vulpiani, "Ergodic observables in nonergodic systems: The example of the harmonic chain," Physica A: Statistical Mechanics and its Applications **630**, 129273 (2023).
[5] A. Santoro, F. Battiston, M. Lucas, G. Petri, and E. Amico, "Higher-order connectomics of human brain function reveals local topological signatures

ACCEPTED MANUSCRIPT
Chaos
An Interdisciplinary Journal
of Nonlinear Science
AIP Publishing
This is the author's peer reviewed, accepted manuscript. However, the online version of record will be different from this version once it has been copyedited and typeset.
PLEASE CITE THIS ARTICLE AS DOI: 10.1063/5.0318179

of task decoding, individual identification, and behavior," Nature Communications **15**, 10244 (2024).
[6]G. Petri, P. Expert, F. Turkheimer, R. Carhart-Harris, D. Nutt, P. J. Hellyer, and F. Vaccarino, "Homological scaffolds of brain functional networks," Journal of The Royal Society Interface **11**, 20140873 (2014).
[7]C. J. Honey, R. Kötter, M. Breakspear, and O. Sporns, "Network structure of cerebral cortex shapes functional connectivity on multiple time scales," Proceedings of the National Academy of Sciences **104**, 10240–10245 (2007).
[8]A. Patania, G. Petri, and F. Vaccarino, "The shape of collaborations," EPJ Data Science **6**, 18 (2017).
[9]M. Ye, L. Zino, Z. Mlakar, J. W. Bolderdijk, H. Risselada, B. M. Fennis, and M. Cao, "Collective patterns of social diffusion are shaped by individual inertia and trend-seeking," Nature Communications **12**, 5698 (2021).
[10]C. Castellano, S. Fortunato, and V. Loreto, "Statistical physics of social dynamics," Reviews of Modern Physics **81**, 591–646 (2009).
[11]D. Centola and M. Macy, "Complex contagions and the weakness of long ties," American Journal of Sociology **113**, 702–734 (2007).
[12]G. Cencetti, F. Battiston, B. Lepri, and M. Karsai, "Temporal properties of higher-order interactions in social networks," Scientific Reports **11**, 7028 (2021).
[13]A. Antelmi, G. Cordasco, C. Spagnuolo, and P. Szufel, "Social influence maximization in hypergraphs," Entropy **23**, 796 (2021).
[14]S. Arya, A. B. George, and J. P. O'Dwyer, "Sparsity of higher-order landscape interactions enables learning and prediction for microbiomes," Proceedings of the National Academy of Sciences **120**, e2307313120 (2023).
[15]J. Friedman, L. M. Higgins, and J. Gore, "Community structure follows simple assembly rules in microbial microcosms," Nature Ecology & Evolution **1**, 0109 (2017).
[16]J. M. Levine, J. Bascompte, P. B. Adler, and S. Allesina, "Beyond pairwise mechanisms of species coexistence in complex communities," Nature **546**, 56–64 (2017).
[17]S. Cui, Q. Zhao, G. Zhang, H. Jardon-Kojakhmetov, and M. Cao, "Analysis of higher-order Lotka-Volterra models: Application of S-tensors and the polynomial complementarity problem," IEEE Transactions on Automatic Control , 1–16 (2025).
[18]M. Tyloo and R. Delabays, "System size identification from sinusoidal probing in diffusive complex networks," Journal of Physics: Complexity **2**, 025016 (2021).
[19]M. Porfiri, "Validity and limitations of the detection matrix to determine hidden units and network size from perceptible dynamics," Physical Review Letters **124**, 168301 (2020).
[20]X. Tang, W. Huo, Y. Yuan, X. Li, L. Shi, H. Ding, and J. Kurths, "Dynamical network size estimation from local observations," New Journal of Physics **22**, 093031 (2020).
[21]P. De Lellis and M. Porfiri, "Inferring the size of a collective of self-propelled Vicsek particles from the random motion of a single unit," Communications Physics **5**, 86 (2022).
[22]L. Neuhäuser, M. Scholkemper, F. Tudisco, and M. T. Schaub, "Learning the effective order of a hypergraph dynamical system," Science Advances **10**, eadh4053 (2024).
[23]H. Haehne, J. Casadiego, J. Peinke, and M. Timme, "Detecting hidden units and network size from perceptible dynamics," Physical Review Letters **122**, 158301 (2019).
[24]R. Succar, A. Boldini, and M. Porfiri, "Detecting hidden states in stochastic dynamical systems," Physical Review Research **6**, 013149 (2024).
[25]R. E. Kalman, "On the general theory of control systems," in *Proceedings of the First International Conference on Automatic Control* (IFAC, Moscow, USSR, 1960) pp. 481–493.
[26]P. Celli and M. Porfiri, "The detection matrix as a model-agnostic tool to estimate the number of degrees of freedom in mechanical systems and engineering structures," Chaos: An Interdisciplinary Journal of Nonlinear Science **32**, 033106 (2022).
[27]G. Börner, H. Haehne, J. Casadiego, and M. Timme, "Revealing system dimension from single-variable time series," Chaos: An Interdisciplinary Journal of Nonlinear Science **33** (2023).
[28]S. Boccaletti, P. De Lellis, C. Del Genio, K. Alfaro-Bittner, R. Criado, S. Jalan, and M. Romance, "The structure and dynamics of networks with higher order interactions," Physics Reports **1018**, 1–64 (2023).
[29]L. Gallo, R. Muolo, L. V. Gambuzza, V. Latora, M. Frasca, and T. Carletti, "Synchronization induced by directed higher-order interactions," Communications Physics **5**, 263 (2022).
[30]R. Lambiotte, M. Rosvall, and I. Scholtes, "From networks to optimal higher-order models of complex systems," Nature Physics **15**, 313–320 (2019).
[31]F. Battiston, G. Cencetti, I. Iacopini, V. Latora, M. Lucas, A. Patania, J.-G. Young, and G. Petri, "Networks beyond pairwise interactions: Structure and dynamics," Physics Reports **874**, 1–92 (2020).
[32]F. Battiston, E. Amico, A. Barrat, G. Bianconi, G. Ferraz de Arruda, B. Franceschiello, I. Iacopini, S. Kéfi, V. Latora, Y. Moreno, M. M. Murray, T. P. Peixoto, F. Vaccarino, and G. Petri, "The physics of higher-order interactions in complex systems," Nature Physics **17**, 1093–1098 (2021).
[33]S. Majhi, M. Perc, and D. Ghosh, "Dynamics on higher-order networks: a review," Journal of The Royal Society Interface **19**, 20220043 (2022).
[34]J. Pickard, A. Surana, A. Bloch, and I. Rajapakse, "Observability of hypergraphs," in *Proceedings of the 62nd IEEE Conference on Decision and Control* (Marina Bay Sands, Singapore, 2023) p. 2445–2451.
[35]X.-J. Xu, S. He, and L.-J. Zhang, "Dynamics of the threshold model on hypergraphs," Chaos: An Interdisciplinary Journal of Nonlinear Science **32**, 023125 (2022).
[36]D. Schlager, K. Clauß, and C. Kuehn, "Stability analysis of multiplayer games on adaptive simplicial complexes," Chaos: An Interdisciplinary Journal of Nonlinear Science **32**, 053128 (2022).
[37]C. Zhang, H. Yang, S. Cui, B. Jiang, and M. Cao, "Global and local observability of hypergraphs," arXiv preprint arXiv:2402.00078 (2024).
[38]R. Delabays, G. De Pasquale, F. Dörfler, and Y. Zhang, "Hypergraph reconstruction from dynamics," Nature Communications **16**, 2691 (2025).
[39]In principle, global differentiability can be relaxed in favor of local differentiability in the neighborhood of a nominal trajectory.
[40]A. Isidori, *Nonlinear Control Systems*, 3rd ed. (Springer, London, UK, 1999).
[41]J. Mathews and R. L. Walker, *Mathematical Methods of Physics*, 2nd ed. (W.A. Benjamin, San Francisco CA, US, 1970).
[42]W. J. Rugh, *Lynear System Theory*, 2nd ed. (Pearson, London, UK, 1996) Chap. 9.
[43]F. Lo Iudice, F. Sorrentino, and F. Garofalo, "On node controllability and observability in complex dynamical networks," IEEE Control Systems Letters **3**, 847–852 (2019).
[44]G. Reissig, C. Hartung, and F. Svaricek, "Strong structural controllability and observability of linear time-varying systems," IEEE Transactions on Automatic Control **59**, 3087–3092 (2014).
[45]E. D. Sontag, *Mathematical Control Theory*, 2nd ed. (Springer, New York NY, US, 1998).
[46]V. Thibeault, A. Allard, and P. Desrosiers, "The low-rank hypothesis of complex systems," Nature Physics **20**, 294–302 (2024).
[47]This claim can be proved by computing the norm of the right and side of (6) , applying the triangle inequality, and the norm submultiplicativity.
[48]G. Benettin, L. Galgani, A. Giorgilli, and J.-M. Strelcyn, "Lyapunov characteristic exponents for smooth dynamical systems and for hamiltonian systems; a method for computing all of them. part 1: Theory," Meccanica **15**, 9–20 (1980).
[49]J. P. Eckmann and D. Ruelle, "Ergodic theory of chaos and strange attractors," Reviews of Modern Physics **57**, 617–656 (1985).
[50]L.-S. Young, "Mathematical theory of lyapunov exponents," Journal of Physics A: Mathematical and Theoretical **46**, 254001 (2013).
[51]J. MacQueen, "Some methods for classification and analysis of multivariate observations," in *Proceedings of the Fifth Berkeley Symposium on Mathematical Statistics and Probability* (University of California, Berkeley, US, 1967) pp. 281–297.
[52]Y.-Y. Liu, J.-J. Slotine, and A.-L. Barabási, "Observability of complex systems," Proceedings of the National Academy of Sciences **110**, 2460–2465 (2013).
[53]A. Braunstein, L. Dall'Asta, G. Semerjian, and L. Zdeborová, "Network dismantling," Proceedings of the National Academy of Sciences **113**, 12368–12373 (2016).